We are IntechOpen, the world's leading publisher of Open Access books Built by scientists, for scientists

6,900
Open access books available

186,000
International authors and editors

200M
Downloads

Our authors are among the

154
Countries delivered to

TOP 1%
most cited scientists

12.2%
Contributors from top 500 universities

WEB OF SCIENCE™

Selection of our books indexed in the Book Citation Index
in Web of Science™ Core Collection (BKCI)

Interested in publishing with us?
Contact book.department@intechopen.com

Growth Mode and Characterization of Si/SiC Heterostructure of Large Lattice-Mismatch

Lianbi Li

Additional information is available at the end of the chapter

Abstract

The Si/6H-SiC heterostructure of large lattice mismatch follows domain epitaxy mode, which release most of the lattice-mismatch strain, and the coherent Si epilayers can be grown on 6H-SiC. An interfacial misfit dislocation array is present at the interface that determines the domain's size. In this chapter, transmission electron microscopy (TEM) and high resolution X-ray diffraction (HRXRD) were employed to reveal in-plane orientation, interface structure and growth mode of the Si/SiC heterostructure. Based on the characterizations, residual lattice mismatch and edge misfit dislocation density at the hetero-interface can be precisely controlled. And these characterization methods are applicable for the heterostructures of large-lattice mismatch, except for the heterostructures with different crystal symmetry on the film and the substrate.

Keywords: large lattice mismatch, domain matching mode, SiC-based heterostructure, in-plane orientation, Interface micro-structure

1. Introduction

With advantageous material properties such as a wide bandgap and high thermal conductivity, silicon carbide (SiC) has attracted much attention for its wide applications in the photoelectric devices of high temperature and high power [1–5]. However, due to the wide bandgap, SiC-based photoelectric devices can be only driven by ultraviolet (UV) light, which essentially limits the application of visible and infrared light detection. Si/SiC heterostructure is suggested to make SiC-based devices to be light-activated by non-UV light, in which Si is used as a non-UV light absorption layer [6, 7]. In our previous work, it was found that the Si films on SiC substrates always have a polycrystalline structure with multiple orientations, while the preferential growth of the Si films with different orientations can be obtained at different growth

temperature [8–12]. The interface-structure of the heterostructure determines some important parameters such as the preferential orientation [13, 14], the interface state density [15–17] and the carrier mobility, which have significant impact on the heterostructure device performance. By observation of the Si/SiC interface-structure with different growth temperatures, the growth mode of the Si/SiC heterostructure can be revealed, and the accurate control of the growth orientation may be achieved. At present, the studies of the SiC-based Si/SiC heterostructure just focused on the electrical performance of the heterostructures in SiC SBD [18] and SiC MOSFET [19, 20], the growth mode and interface-structure of the Si/SiC heterostructure is rarely reported.

2. Growth mode, interface micro-structure and in-plane orientation of the Si/SiC heterostructure

2.1. Growth mode of the heterostructures of large lattice-mismatch

The crystal structure of Si and 6H-SiC is face-centered cubic (FCC) and hexagonal close-packed (HCP) with in-plane lattice constants of $a_{Si} = 5.430$ Å and $a_{SiC} = 3.081$ Å, respectively. The lattice mismatch of the Si(111)/6H-SiC(0001) is as large as 19.8%, which is given by

$$\varepsilon_x = \varepsilon_y = \left(a_{sic(0001)} - a_{Si(111)}\right)/a_{Si(111)} \tag{1}$$

where $a_{sic(0001)}$ and $a_{Si(111)}$ are the lattice constants of the SiC(0001) and Si(111) crystalline planes, respectively. If the lattice mismatch of the heterostructure is sufficiently low, the mismatch strain can be released by interfacial atomic relaxation of the heterostructure, and the strained-layer heterostructure with no interfacial misfit dislocations (MD) will be attained. However, the Si/SiC heterostructure has a large lattice mismatch, the epitaxial growth is still followed except that domain matching (DM) mode [21] in order to reduce the mismatch, and therefore an interfacial MD array is present at the interface that determines the domain's size [22–26]. A schematic illustration of mechanisms for accommodation of lattice mismatch strain in large-mismatch systems with domain epitaxial growth is shown in **Figure 1**. And this matching mode is applicable for the heterostructures with similar crystal symmetry on the film and the substrate. In the Si/6H-SiC system, domains consisting of m lattice constants of the Si film match with n of the SiC substrate. During domain matching system, the domain size na_{sic} of the SiC substrate does not match perfectly with ma_{Si} of the Si film and thus a residual domain mismatch strain is present in the film in the x direction, given by

$$\varepsilon_x = (ma_{sic\,x} - na_{Si\,x})/na_{Si\,x} \tag{2}$$

Similarly, the residual strain

$$\varepsilon_y = \left(pa_{sic\,y} - qa_{Si\,y}\right)/qa_{Si\,y} \tag{3}$$

where p and q are integers, is present in the y direction. The lattice-mismatch of the Si/6H-SiC heterostructure calculated with the DM mode are very small, the coherent Si epilayer can be
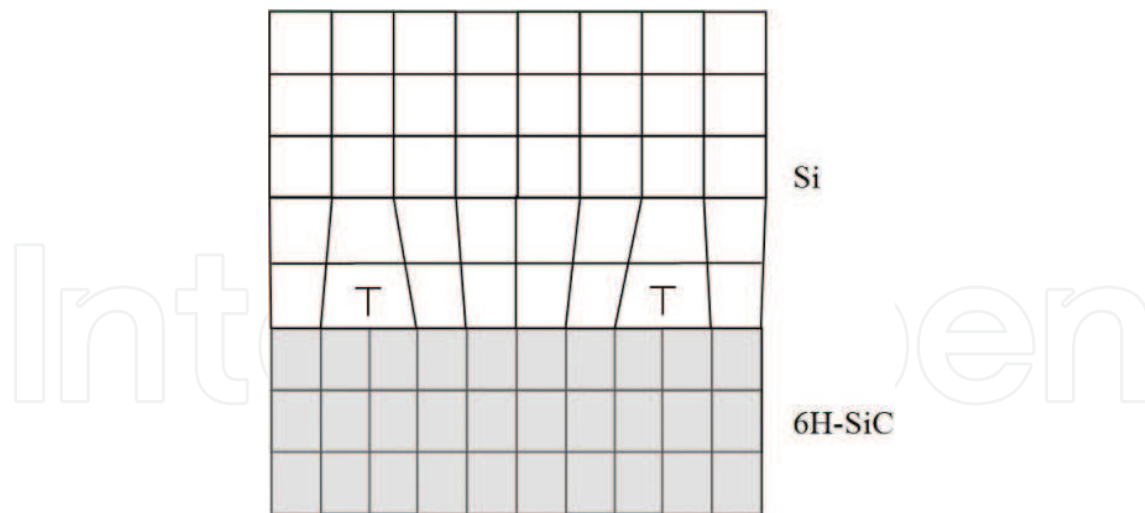
Figure 1. Schematic illustration of mechanisms for accommodation of lattice mismatch strain in large mismatch systems with DM mode.

grown on 6H-SiC. This type of edge misfit dislocation is also observed in other heterostructure of large lattice-mismatch, such as TiN/Si [23], ZnO/α-Al$_2$O$_3$ [23], Sc$_2$O$_3$/GaN [24], GaAs/Si [25] and In$_x$Ga$_{1-x}$N/GaN [26].

2.2. Interface micro-structure of the Si/SiC heterostructure

The low magnification cross-sectional transmission electron microscopy (TEM) bright-field image of the Si thin film grown on 6H-SiC(0001) at 900°C is shown in **Figure 2(a)**. In this image, the lower part belongs to the 6H-SiC substrate, while the upper part represents the Si thin film. The Si film with a thickness of about 0.55 μm shows irregular heterogeneous diffraction contrast, which suggests the existence of some structural defects such as stacking faults (SF) and twins in the film, as labeled in **Figure 2(a)**. The selected area electron diffraction (SAED) patterns of the Si/6H-SiC heterostructure corresponding to Si[-110]SiC[-12-10] zone axes are shown in **Figure 2(b)**. It is confirmed that the Si film has epitaxial connection with the 6H-SiC substrate and the orientation relationship of Si/6H-SiC heterostructure is (111)[1-10]$_{Si}$// (0001)[1-210]$_{6H-SiC}$. Alignment of the diffraction spots indicates that FFC-on-HCP epitaxial orientation, i.e., (111)$_{Si}$//(0001)$_{6H-SiC}$ is maintained at a growth temperature of 900°C. It should be pointed out that the extinction diffraction spots of (10-10)$_{SiC}$ and (10-16)$_{SiC}$ can be observed in the SAED patterns because of the multiple diffraction. A superposition of two FCC <110> zone diffraction patterns, which are symmetrical to each other with respect to the (111) mirror plane, indicating that the lamellar structure observed in the film consists of alternate stacks of twins, as shown in **Figure 2(b)**. Furthermore, the faint diffused streaks along the <111> orientation indicate that there exist a large number of SFs. And this agrees with the results of the diffraction contrast study.

Figure 3(a) shows a high-resolution TEM image of the Si/6H-SiC interface, exhibiting interfaces of Si(111)/6H-SiC(0001) without any indication of interfacial reactions, however, it is not crystallographic sharp, which reflects the roughness of the Si layer's surface and the poor
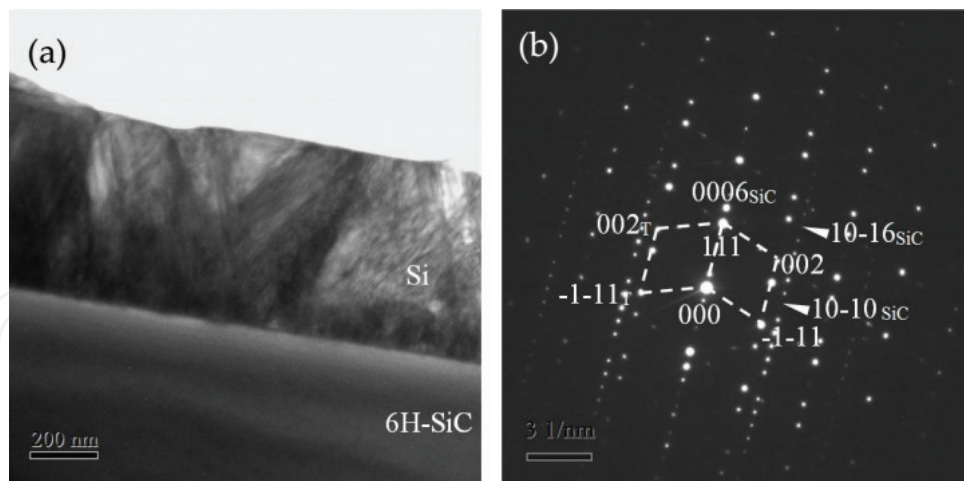
Figure 2. Cross-sectional low magnification TEM image and the SAED patterns of Si films grown on 6H-SiC (0001) at 900°C. (a) TEM image, (b) SAED patterns corresponding to Si[-110]SiC[-12-10] zone axes.

crystallographic match between interatomic distances in close-packed layers of between Si (111) and SiC (0001) planes (in-plane constants 3.84 Å for Si and 3.08 Å for 6H-SiC). Moreover, typical structural defects such as SFs and twins are clearly observed in the Si film, which are labeled in **Figure 3(a)**. **Figure 3(b)** is the magnified image of the region b in **Figure 3(a)**, which further confirms the epitaxial relation of the Si/6H-SiC heterostructure. Fourier-filtering technique is applied to remove the non-periodic information such as background signal and the structural defects in the Si film. The Fourier-filtered high-resolution TEM images of the Si thin film, the 6H-SiC substrate and the Si/6H-SiC interface are shown in **Figure 3(c)–3(e)**, respectively. It is clearly observed that the SiC substrate with the HCP stacking sequence as ABCACB has a crystal plane spacing of 2.57 Å, while the Si film with the FCC stacking as ABC has a crystal plane spacing of 3.21 Å. Calculated from the crystal plane spacing, lattice mismatch of the Si(111)/6H-SiC(0001) heterostructure is about 19.8%, which is in accordance with the calculation results based on the fast-Fourier transform (FFT) pattern. Nevertheless, the (0001) lattice planes of SiC and (111) lattice planes of Si are well aligned, and the Si film grows epitaxially but with MDs (indicated by the arrows) at the interface between the Si film and the 6H-SiC substrate, which can be easily identified by extra lattice fringes in the 6H-SiC. The Si epitaxial growth follows the DM mode, every five 6H-SiC(1-210) planes match with four Si (1-10) planes along the interface, as shown in **Figure 3(e)**. Moreover, the invariant crystal plane spacings of the Si film and the 6H-SiC substrate at the Si/6H-SiC interface demonstrate that the interfacial MD array accommodates most of the lattice mismatch strain and makes the lattice coincident at the Si/6H-SiC interface.

Based on the results shown above, the in-plane orientation of the $(111)_{Si}//(0001)_{6H-SiC}$ heterostructure is schematically shown in **Figure 4(a)**. Both of the 6H-SiC(0001) and Si(111) lattice planes have the same triangular lattice in two-dimensions (2D). And the Si(111) layers epitaxially grow on 6H-SiC(0001) without rotation of the 2D triangular lattice. However, the in-plane lattice constant of the Si(111) (3.84 Å) is larger than that of the 6H-SiC(0001) (3.08 Å), as shown in **Figure 4(b)**. The FCC-on-HCP epitaxial relationship with a four-to-five mode of Si-to-SiC is clearly observed. The residual mismatch calculated by the DM mode is only 0.26%,
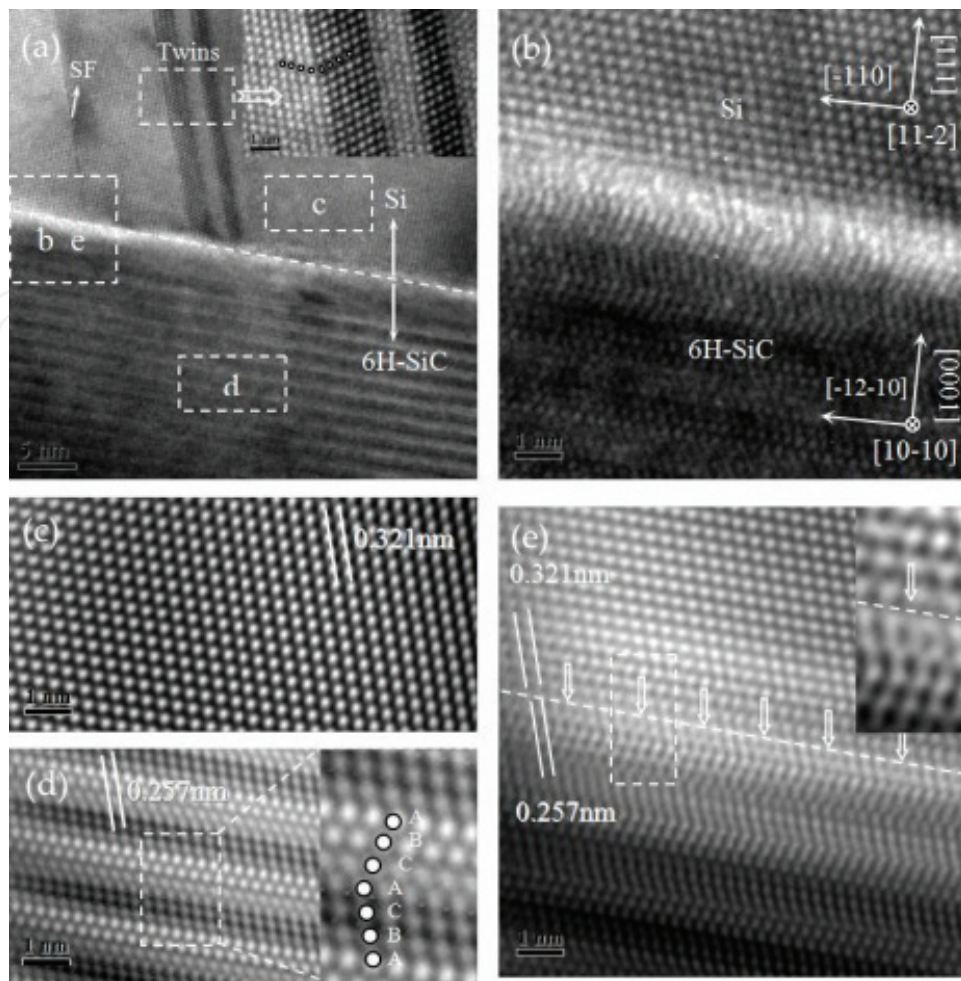
Figure 3. A HRTEM image of the Si/6H-SiC heterojunction grown at 900°C (a), a magnified image (b), and the Fourier-filtered HRTEM images (c)–(e).

which is much smaller than the mismatch of 19.8% calculated by the conventional lattice matching (LM) mode. Because the 2D triangular lattice of the Si(111) film has no rotation during epitaxial growth on 6H-SiC(0001), the domain mismatch strain ε_x in the x direction and ε_y in the y direction are the same as 0.26%.

XRD data, shown elsewhere [9], indicates that the Si phase with [110] orientation appears when the temperature increases higher than 1000°C, which is confirmed by the TEM characterizations. **Figure 5(a)** is a low magnification cross-sectional TEM image of the Si/6H-SiC(0001) heterostructure grown at 1050°C. The Si/SiC heterostructure has a sharp interface and consist of columnar grains. SAED patterns at the Si/6H-SiC interface corresponding to Si[-110]SiC[1-210] zone axes in **Figure 5(b)** clearly show the FCC-on-HCP orientation relationship of (110)[001]$_{Si}$//(0001)[10-10]$_{6H-SiC}$, confirming the epitaxial growth of the Si films with [110] orientation. The high-resolution TEM image of the Si(110)/SiC(0001) heterostructure is shown in **Figure 6(a)**. The Si/SiC interface is crystallographic sharp without any indication of the interfacial reaction products. **Figure 6(b)** is the Fourier-filtered HRTEM image, which confirms the epitaxial connection of the Si/6H-SiC heterostructure. Calculated from the crystal plane
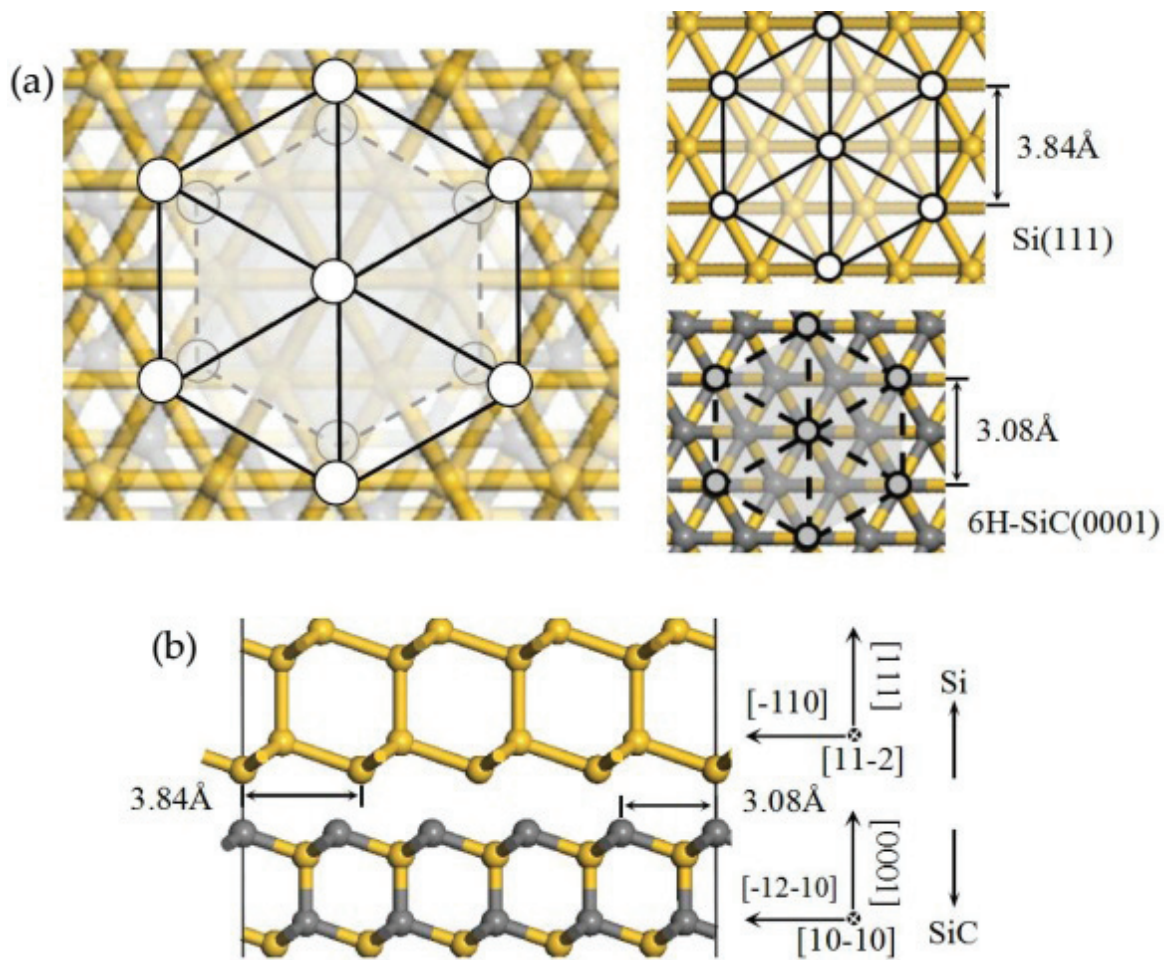
Figure 4. Schematic diagrams of the of Si(111)/6H-SiC(0001) heterojunction. (a) In-plane orientation, (b) atomic structure at the hetero-interface. The insets show the atomic structures of the Si(111) and 6H-SiC(0001) planes.
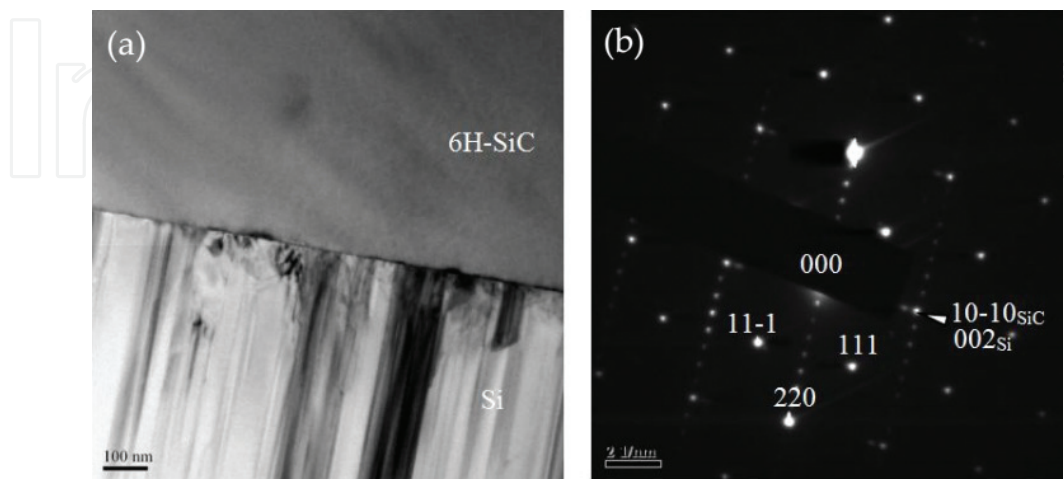

Figure 5. Low magnification cross-sectional TEM image and the SAED patterns of Si films grown on 6H-SiC(0001) at 1050°C. (a) TEM image, (b) SAED patterns of the Si/SiC interface corresponding to Si[-110]SiC[1-210] zone axes.
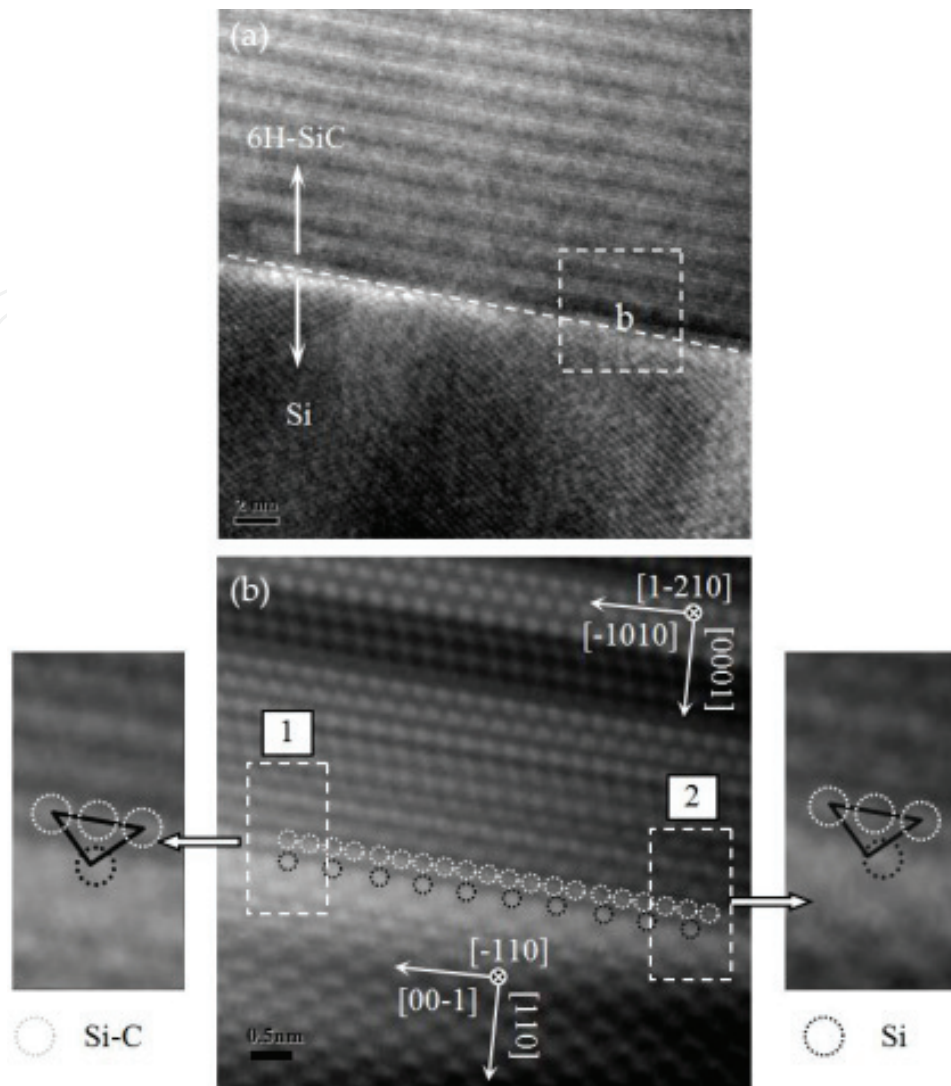
Figure 6. A HRTEM image of the Si/6H-SiC heterojunction grown at 1050°C (a), the Fourier-filtered HRTEM images (b). The insets are the magnified images of region 1 and 2, which show the atomic position of the Si/6H-SiC interface. The atomic positions of Si are slightly different in two regions. It suggests that the Si-to-SiC matching mode at the interface is long-periodic and is merely approximate 1:2.

spacings and the FFT patterns, lattice mismatch of the Si(110)/6H-SiC(0001) heterostructure is 1.84%. The interfacial MD array can also be observed by extra lattice fringes in the 6H-SiC. Every two 6H-SiC(10-10) planes match with one Si(001) planes along the interface, as shown in **Figure 6(b)**. Compared with the Si(111)/6H-SiC(0001) heterostructure with a residual mismatch of 0.26%, the Si(110)/6H-SiC(0001) heterostructure has higher residual mismatch of 1.84% along Si[001]SiC[10-10] orientation. If the Si-to-SiC matching mode is not 1:2 but a long-period structure of 53:54, the lattice mismatch can decrease to −0.55%. Of course the long-period matching is very difficult to be confirmed by experimental observations; however, the trend of this large-period matching can be observed in **Figure 6(b)**. The atomic position of Si in region 1 is slightly different from that of Si in region 2, as shown in the insets. It is suggested that the Si-to-SiC matching at the interface is merely approximate 1:2.

Figure 7(a) shows a HRTEM image of the Si(110)/6H-SiC(0001) interface. Because the observation orientation is SiC[-1010], the 6H stacking sequence as ABCACB of 6H-SiC is not observed. The SAED patterns at the Si/6H-SiC interface corresponding to Si[00-1]SiC[-1010] zone axes are shown in **Figure 7(b)**. SAED patterns at the Si/6H-SiC interface clearly show the FCC-on-HCP orientation relationship of (110)[-110]Si//(0001)[1-210]6H-SiC, confirming the epitaxial growth of the Si films with [110] growth orientation. **Figure 7(c)** shows the Fourier-filtered image of region 1, which further confirms the epitaxial connection of the Si(110)/6H-SiC(0001) heterostructure. The crystal plane spacing at the Si/6H-SiC interface also has no significant change. The Si epitaxial growth follows the DM mode, every five 6H-SiC(1-210) planes match with four Si(-110) planes along the interface, as shown in **Figure 7(d)**. According to the extra SiC lattice planes at the hetero-interface, Burgers vectors of the MDs can be determined uniquely. The MDs are of the pure edge type with a Burgers vector of $\langle 1-210 \rangle_{SiC}/3$ parallel to the interface, which are labeled in **Figure 7(d)**.
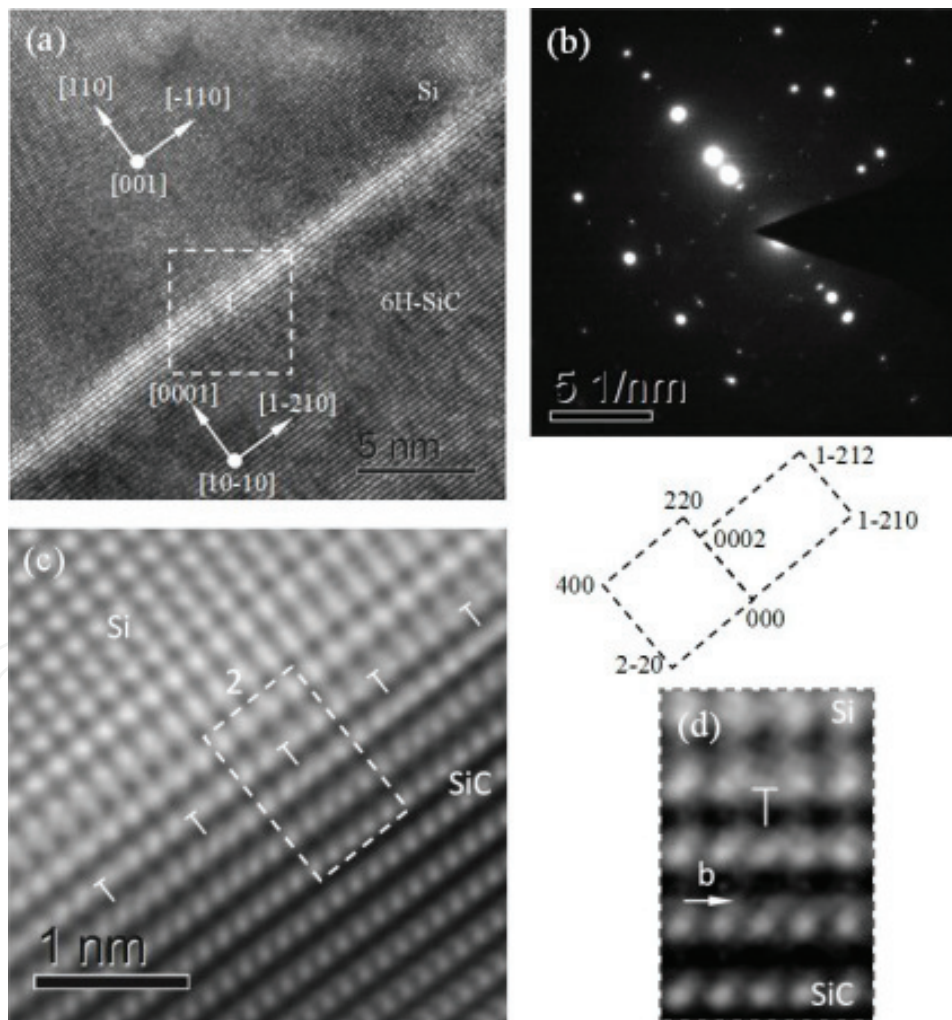

Figure 7. HRTEM images and the SAED patterns of Si(110)/6H-SiC(0001) interface. HRTEM image of the Si(110)/6H-SiC(0001) interface (a), SAED patterns (b), the Fourier-filtered HRTEM images of region 1 (c) and region 2 (d). The SAED patterns at the Si/6H-SiC interface corresponding to Si[00-1]SiC[-1010] zone axes.

Base on the HRTEM observations and SAED analysis, the lattice-structure model of the Si (110)/6H-SiC(0001) heterostructure is constructed and schematically shown in **Figure 8**. It is known that the Si(110) plane has a rectangular 2D lattice with different in-plane constants of 5.43 Å and 3.84 Å along the vertical orientations Si[001] and Si[-110], which is different from the 2D triangular lattice of the 6H-SiC(0001). However, the triangular lattice of 6H-SiC(0001) can be transformed to rectangular 2D lattice by missing partial Si-C atoms, which has in-plane constants of 5.33 Å and 3.08 Å along SiC[10-10] and SiC[1-210] respectively, as shown in **Figure 8(a)**. Along Si[001]SiC[10-10] orientations, the heterostructure has a lattice mismatch of 1.84% with in-plane constants 5.43 Å for Si and 5.33 Å for 6H-SiC. The residual lattice mismatch strain can be released by interfacial atomic relaxation of the Si/6H-SiC heterostructure and the strained-layer with no MDs will be attained. However, the 2D rectangular lattice of 6H-SiC(0001) is converted from the triangular lattice by missing every other Si-C atoms along [10-10] orientation. Therefore, MDs are still present at the Si(110)/6H-SiC(0001) interface and 1:2 mode of Si-to-SiC is observed. Along the vertical orientations Si[-110]SiC[1-210], the Si (110)/6H-SiC(0001) heterostructure has in-plane constants 3.84 Å for Si and 3.08 Å for 6H-SiC, and the interface with a four-to-five mode of Si-to-SiC is shown in **Figure 8(c)**, which is identical with the Si(111)/6H-SiC(0001) heterostructure.
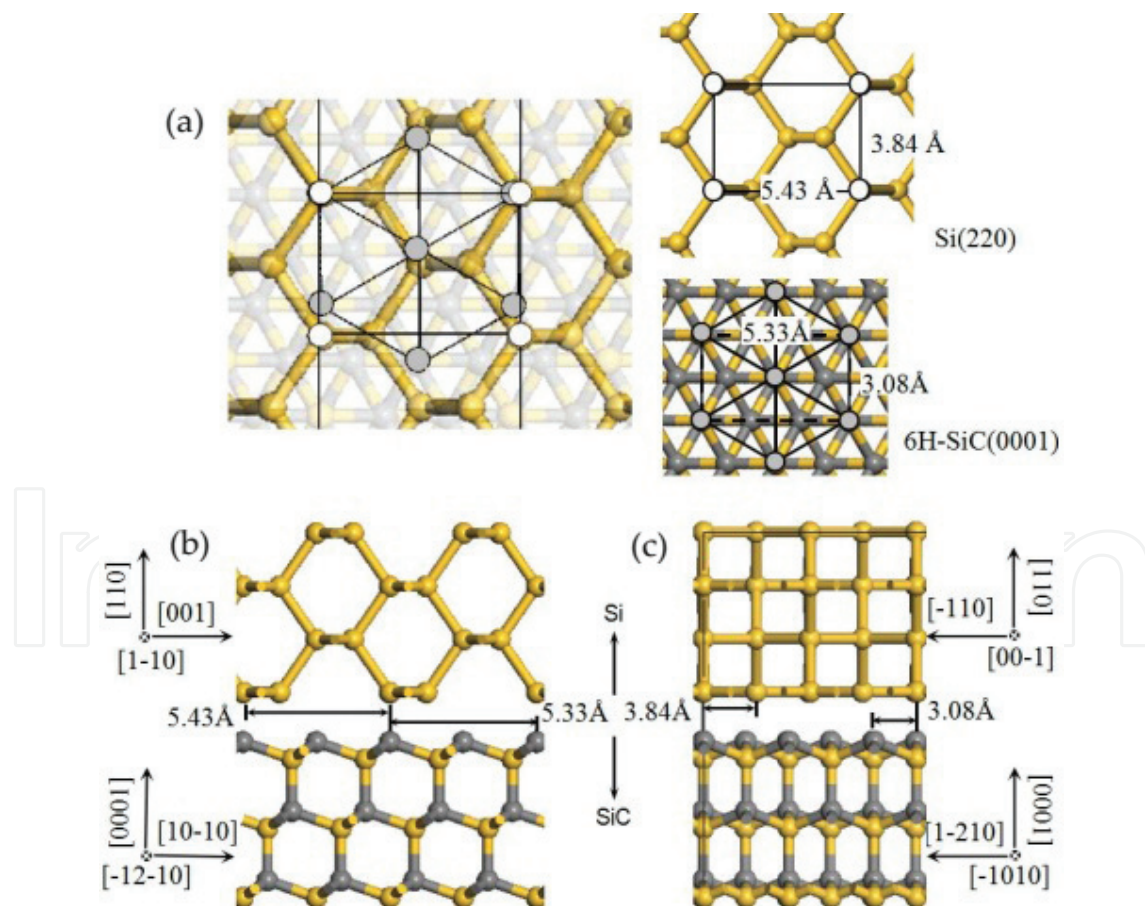

Figure 8. Schematic diagrams of the of Si(110)/SiC(0001) heterojunction. In-plane orientation (a), atomic structure at the interface along Si[001]SiC[10-10] (b) and Si[-110]SiC[1-210] (c). The insets show the atomic structures of the Si(110) and 6H-SiC(0001) planes.

Because of the large lattice mismatch strain, the conventional LM epitaxy is not expected. The lattice mismatch between 6H-SiC and Si is totally accommodated by MDs rather than by uniform elastic strains, the DM mode is observed.

2.3. In-plane orientation of the Si/SiC heterostructure

Figure 9 shows the XRD θ-2θ scans for Si/SiC(0001) heterostructures prepared at 900°C and 1050°C, respectively. It is shown that the Si film is [111] oriented when the Si layer is deposited at the lower temperatures of 900°C, as the growth temperature increase to 1050°C, the Si layer is mainly [110] oriented, which agrees with the SAED characterizations.

The in-plane orientation at the hetero-interface was carefully examined using X-ray phi(φ) scan. For investigating the [11-2] orientation in Si(111) plane, the out-of-plane orientation [110] must be confirmed, as demonstrated in **Figure 10**. **Figure 11(a)** shows XRD 360° φ scans of the Si(110) (χ = 35.27°) reflections of Si(111)/6H-SiC(0001) heterostructure grown at 900°C. Moreover, for investigating [10-10] orientation in 6H-SiC(0001) plane, the φ scans from the 6H-SiC(10-11) (χ = 80°) reflections are also characterized. Narrow and intense peaks with six-fold symmetry are observed. On the basis of the Si(110) and 6H-SiC(10-11) reflections shown in **Figure 11(a)**, it can be concluded that a FCC-on-HCP parallel epitaxy is achieved at 900°C and the in-plane orientation relationship is $(111)[1-10]_{Si}//(0001)[1-210]_{6H-SiC}$. The in-plane orientation of the Si(110)/6H-SiC(0001) heterostructure grown at 1050°C is also characterized, as shown in **Figure 11(b)**. For investigating the [001] orientation in Si(110) plane, the out-of-plane orientation [111] is confirmed firstly. The six-fold symmetry is also observed. It is confirmed that the in-plane orientation relationship is $(110)[001]_{Si}//(0001)[10-10]_{6H-SiC}$.

By means of the in-plane orientation characterizations, the 3D Si/SiC(0001) hetero-interface structures with different orientations are confirmed and schematically shown in **Figure 12**. The Si(111) layers grow epitaxially on 6H-SiC(0001) with an in-plane orientation relationship of Si [11-2]//SiC[10-10], as shown in **Figure 12(a)**. As mentioned above, the Si(111)/SiC(0001) heterostructure follows DM mode, the epitaxial growth is described by 4 (111) interatomic distances of Si matching with 5 (0001) interatomic distances of 6H-SiC, which releases most of the lattice-mismatch strain. The 4:5 matching generates edge-MD array at the Si/6H-SiC interface [13], and the MD density can be calculated as 4.87×10^{13} cm^{-2} according to the model
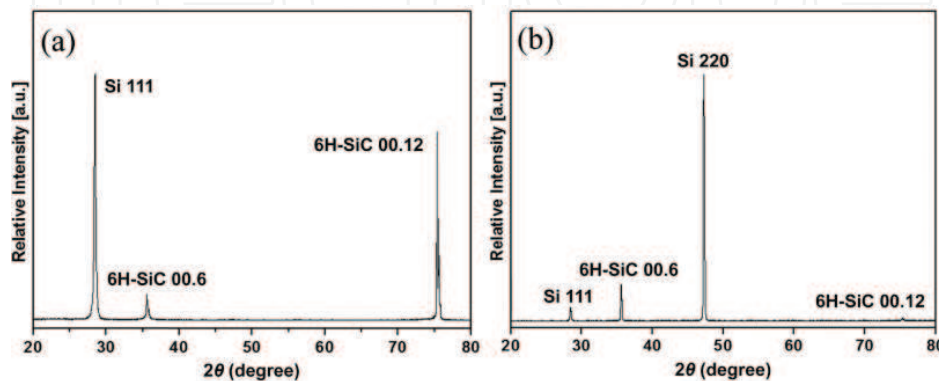

Figure 9. X-ray θ-2θ scans for Si/SiC(0001) heterostructures with the Si layer grown at (a) 900°C and (b) 1050°C.
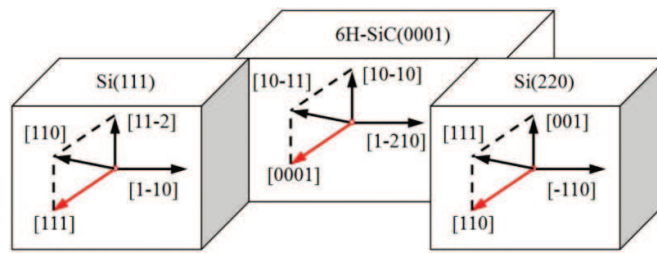
Figure 10. XRD φ scans schematic diagrams of the Si(111)/6H-SiC(0001) and Si(110)/6H-SiC(0001) heterostructures. For investigating the in-plane orientations, at least one out-of-plane orientation needs to be confirmed firstly.
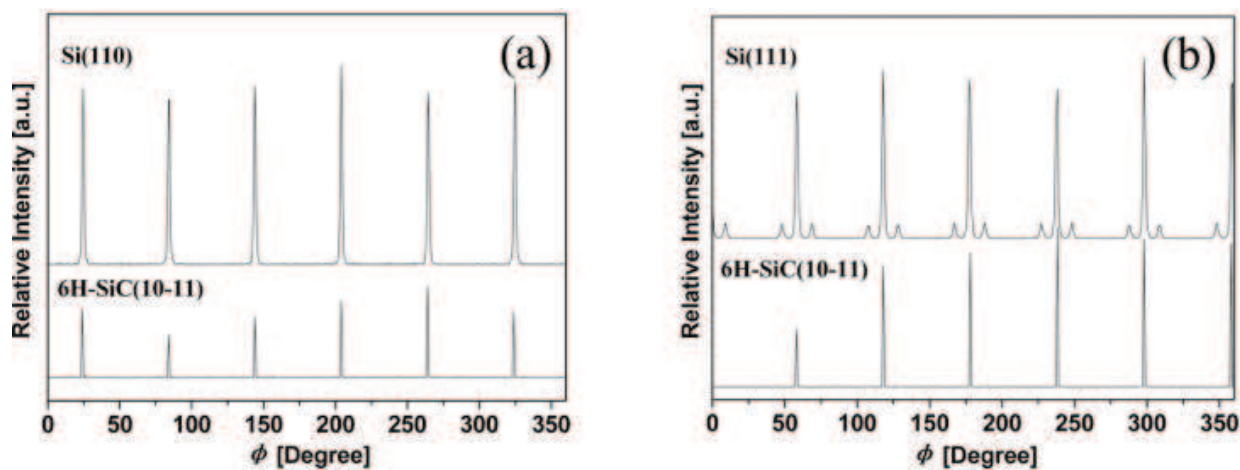

Figure 11. XRD φ scans of the Si/6H-SiC heterostructures, (a) Si(110) (χ = 35.27°) reflections of Si(111)/6H-SiC(0001) heterostructure grown at 900°C, (b) Si(111) (χ = 35.27°) reflections of Si(110)/6H-SiC(0001) heterostructure grown at 1050°C. The φ scans from the 6H-SiC(10-11) (χ = 80°) reflections is also shown as reference at the bottom.

shown in **Figure 12(a)**, which is much smaller than the theoretical value (4.34×10^{14} cm^{-2}). However, the domain size na_{sic} of the SiC substrate (n = 5) does not match perfectly with ma_{Si} of the Si film (m = 4), and thus a residual domain mismatch strain ε, given by Eq. (2) is present in the film. The residual mismatch strain ε of the Si(111)/6H-SiC(0001) heterostructure calculated with the DM mode is 0.26%, which is much smaller than conventional LM mode (19.8%). The Si(110) layers epitaxial grow on 6H-SiC(0001) with an in-plane orientation of Si[-110]//SiC [1-210], and the crystal structure model is schematically shown in **Figure 12(b)**. Along orientations Si[-110]SiC[1-210], the Si(110)/6H-SiC(0001) heterostructure has in-plane constants 3.84 Å for Si and 3.08 Å for 6H-SiC, and the interface with a four-to-five mode of Si-to-SiC is identical with the Si(111)/6H-SiC(0001) heterostructure. Along the vertical Si[001]SiC[10-10] orientations, the distinct 1:2 matching is observed and thus MDs are still present at the Si(110)/6H-SiC(0001) interface. The MD density increases to 1.217×10^{14} cm^{-2} correspondingly, which is still smaller than the theoretical value (2.57×10^{14} cm^{-2}). The heterostructure has a residual mismatch strain ε of 1.84% with in-plane constants 5.43 Å for Si and 5.33 Å for 6H-SiC (**Table 1**).
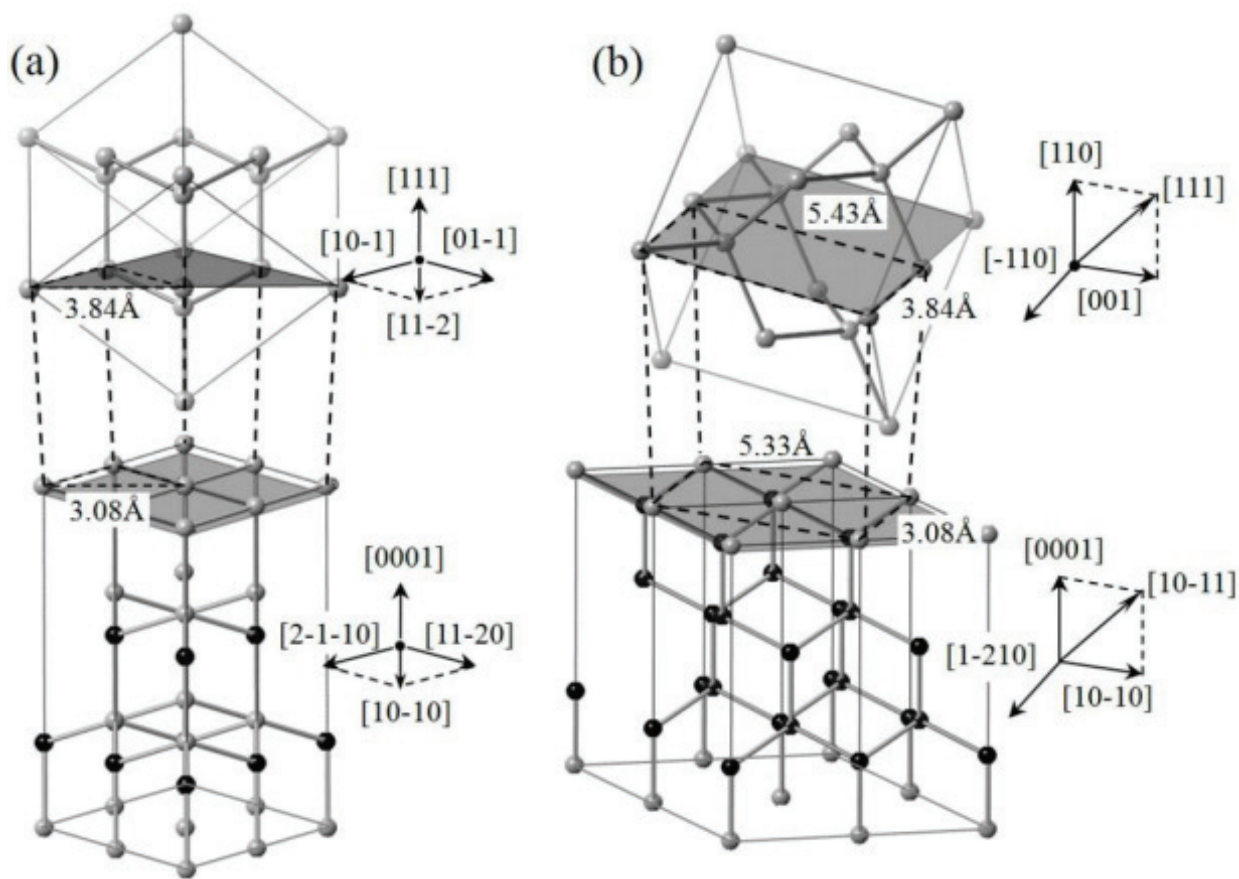
Figure 12. Schematic diagrams of the Si/6H-SiC(0001) heterojunction. Si/6H-SiC heterostructure with the [111] preferential orientation (a), Si/6H-SiC heterostructure with the [110] preferential orientation (b). As the preferential orientations are [111] and [110], the in-plane orientations are Si[01-1]//SiC[11-20] and Si[001]//SiC[10-10], respectively.

Growth orientation	Si-to-SiC DM mode		Residual mismatch		MD density theoretical value	MD density DM mode
Si(111)/6H-SiC(0001)	Si[11-2] SiC [10-10]	Si[1-10] SiC [1-210]	Si[11-2] SiC [10-10]	Si[1-10] SiC [1-210]	4.34×10^{14} cm^{-2}	0.487×10^{14} cm^{-2}
	4:5	4:5	0.26%	0.26%		
Si(110)/6H-SiC(0001)	Si[001] SiC [10-10]	Si[-110] SiC [1-210]	Si[001] SiC [10-10]	Si[-110] SiC [1-210]	2.57×10^{14} cm^{-2}	1.217×10^{14} cm^{-2}
	1:2	4:5	1.84%	0.26%		

The lattice-mismatch of the Si/6H-SiC heterostructure calculated with the domain matching model.

Table 1. Basic semiconductor properties of the Si/6H-SiC interface.

3. Conclusions

In this chapter, Si/SiC heterostructures with different orientations were prepared on 6H-SiC(0001) by LPCVD. The heterostructure of large lattice-mismatch grows by DM mode,

which releases most of the lattice-mismatch strain, and the coherent Si epilayers can be grown on 6H-SiC. Si(111)/6H-SiC(0001) heterostructure obtained at 900°C has an in-plane orientation relationship of $(111)[1\text{-}10]_{Si}//(0001)[1\text{-}210]_{6H\text{-}SiC}$. The Si(111)/6H-SiC(0001) interface has the 4:5 Si-to-SiC matching mode with a residual lattice-mismatch of 0.26% along both the Si[11-2] and Si[1-10] orientations. As the growth temperature increases to 1050°C, the preferential orientation of the Si film transitions to [110]. SAED patterns show that the in-plane orientation relationship is $(110)[001]_{Si}//(0001)[10\text{-}10]_{6H\text{-}SiC}$. Along Si[-110] orientation, the Si-to-SiC matching is still 4:5; along the vertical orientation Si[001], the matching mode is approximate 1:2 and the residual mismatch is 1.84% correspondingly. The atom quantity in one DM period decreases with increasing residual mismatch and vice versa. The Si film epitaxially grows but with MDs at the Si/6H-SiC interface. The MD density of the Si(111)/6H-SiC(0001) and Si(110)/6H-SiC(0001) obtained by experimental observations is as low as 0.487 and 1.217×10^{14} cm^{-2}, respectively, which is much smaller than the theoretical value.

Acknowledgements

Conflict of interest

We declare that we have no financial and personal relationships with other people or organizations that can inappropriately influence our work.

Author details

Lianbi Li[1,2]*

*Address all correspondence to: xpu_lilianbi@163.com

1 School of Science, Xi'an Polytechnic University, Xi'an, China

2 Department of Electronic Engineering, Xi'an University of Technology, Xi'an, China

References

[1] Seely JF, Kjornrattanawanich B, Holland GE, Korde R. Response of a SiC photodiode to extreme ultraviolet through visible radiation. Optics Letters. 2005;**30**:3120-3122. DOI: 10.1364/OL.30.003120

[2] Xin X, Yan F, Koeth TW, Joseph C, Hu J, Wu J, Zhao JH. Demonstration of 4H-SiC visible-blind EUV and UV detector with large detection area. Electronics Letters. 2005;**41**:1192-1193. DOI: 10.1049/el:20052977

[3] Hu J, Xin X, Zhao JH, Yan F, Guan B, Seely J, Kjornrattanawanich B. Highly sensitive visible-blind extreme ultraviolet Ni/4H-SiC Schottky photodiodes with large detection area. Optics Letters. 2006;**31**:1591-1593. DOI: 10.1364/OL.31.001591

[4] Levinshtein ME, Ivanov PA, Agarwal AK, Palmour JW. Optical switch-on of silicon carbide thyristor. Electronics Letters. 2002;**38**:592-593. DOI: 10.1049/el:20020415

[5] Henning JP, Schoen KJ, Melloch MR, Woodall JM, Cooper JA. Electrical characteristics of rectifying polycrystalline silicon/silicon carbide heterojunctions. Journal of Electronic Materials. 1998;**27**:296-299. DOI: 10.1007/s11664-998-0403-x

[6] Li LB, Chen ZM, Ren ZQ, Gao ZJ. Non-UV photoelectric properties of the Ni/n-Si/N$^+$-SiC isotype heterostructure Schottky barrier photodiode. Chinese Physics Letters. 2013;**30**(9): 097304. DOI: 10.1088/0256-307X/30/9/097304

[7] Li LB, Chen ZM, Liu WT, Li WC. Electrical and photoelectric properties of p-Si/n$^+$-6H-SiC heterojunction non-ultraviolet photodiode. Electronics Letters. 2012;**48**:1227-1228. DOI: 10.1049/el.2012.1471

[8] Li LB, Chen ZM, Xie LF, Yang C. TEM characterization of Si films grown on 6H-SiC (0001) C-face. Materials Letters. 2013;**93**:330-332. DOI: 10.1016/j.matlet.2012.11.093

[9] Xie LF, Chen ZM, Li LB, Yang C, He XM, Ye N. Preferential growth of Si films on 6H-SiC(0001) C-face. Applied Surface Science. 2012;**261**:88-91. DOI: 10.1016/j.apsusc.2012. 07.101

[10] Li LB, Chen ZM, Zang Y, Song LX, Han YL, Chu Q. Epitaxial growth of Si/SiC heterostructures with different preferred orientations on 6H-SiC(0001) by LPCVD. CrystEngComm. 2016;**18**:5681. DOI: 10.1039/c6ce00137h

[11] Li LB, Chen ZM, Zang Y, Feng S. Atomic-scale characterization of Si(110)/6H-SiC(0001) heterostructure by HRTEM. Materials Letters. 2016;**163**:47-51. DOI: 10.1016/j.matlet. 2015.10.017

[12] Li LB, Chen ZM, Zang Y. Interface-structure of the Si/SiC heterojunction grown on 6H-SiC. Journal of Applied Physics. 2015;**117**:013104. DOI: 10.1063/1.4901644

[13] Wu WB, Wong KH, Choy CL. Epitaxial growth of SrTiO$_3$ films with different orientations on TiN buffered Si(001) by pulsed laser deposition. Thin Solid Films. 2000;**360**:103-106. DOI: 10.1016/S0040-6090(99)01091-3

[14] Sugawara Y, Shibata N, Hara S, Ikuhara Y. Interface structure of face-centered-cubic-Ti thin film grown on 6H-SiC substrate. Journal of Materials Research. 2000;**15**:2121-2124. DOI: 10.1557/JMR.2000.0305

[15] Wang K, Hattrick-Simpers JR, Bendersky LA. Phase transformation in an yttrium-hydrogen system studied by TEM. Acta Materialia. 2010;**58**:2585-2597. DOI: 10.1016/j. actamat.2009.12.045

[16] Tokuyuki T, Shiro H. Control of interface states at metal/6H-SiC(0001) interfaces. Physical Review B. 2004;**70**:035312. DOI: 10.1103/PhysRevB.70.035312

[17] Long C, Ustin SA, Ho W. Structural defects in 3C-SiC grown on Si by supersonic jet epitaxy. Journal of Applied Physics. 1999;**86**:2509-2515. DOI: 10.1063/1.371085

[18] Pérez-Tomás A, Jennings MR, Davis M, Covington JA, Mawby PA, Shah V, Grasby T. Characterization and modeling of n-n Si/SiC heterojunction diodes. Journal of Applied Physics. 2007;**102**:014505. DOI: 10.1063/1.2752148

[19] Pérez-Tomás A, Jennings MR, Davis M, Shah V, Grasby T, Covington JA, Mawby PA. High doped MBE Si p-n and n-n heterojunction diodes on 4H-SiC. Microelectronics Journal. 2007;**38**:1233-1237. DOI: 10.1016/j.mejo.2007.09.019

[20] Guy OJ, Jenkins TE, Lodzinski M, Castaing A, Wilks SP, Bailey P, Noakes TCQ. Ellipsometric and MEIS studies of 4H-SiC/Si/SiO$_2$ and 4H-SiC/SiO$_2$ interfaces for MOS devices. Materials Science Forum. 2007;**556–557**:509-512. DOI: 10.4028/www.scientific. net/MSF.556-557.509

[21] Tsvetanka Z, Jagannadham K, Narayan J. Epitaxial growth in large-lattice-mismatch systems. Journal of Applied Physics. 1994;**75**:860-871. DOI: 10.1063/1.356440

[22] Narayan J, Tiwari P, Chen X, Chowdhury R, Zheleva T. Epitaxial growth of TiN films on (100) silicon substrates by laser physical vapor deposition. Applied Physics Letters. 1992; **61**:1290-1292. DOI: 10.1063/1.107568

[23] Narayan J, Larson BC. Domain epitaxy: A unified paradigm for thin film growth. Journal of Applied Physics. 2003;**93**:278-285. DOI: 10.1063/1.1528301

[24] Niermann T, Zengler D, Tarnawska L, Stork P, Schroeder T, Lehmann M. Virtual GaN substrates via Sc$_2$O$_3$/Y$_2$O$_3$ buffers on Si(111): Transmission electron microscopy charac- terization of growth defects. Journal of Applied Physics. 2013;**113**:223501. DOI: 10.1063/1. 4809561

[25] Otsuka N, Choi C, Nakamura Y, Nagakura S, Fischer R, Peng CK, Morkog H. High resolution electron microscopy of misfit dislocations in the GaAs/Si epitaxial interface. Applied Physics Letters. 1986;**49**:277-279. DOI: 10.1063/1.97140

[26] Lü W, Li DB, Li CR, Zhang Z. Generation and behavior of pure-edge threading misfit dislocations in In$_x$Ga$_{1-x}$N/GaN multiple quantum wells. Journal of Applied Physics. 2004; **96**:5267-5270. DOI: 10.1063/1.1803633